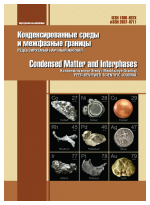

ISSN 1606-867X (Print)
ISSN 2687-0711 (Online)
Condensed Matter and Interphases
Kondensirovannye Sredy i Mezhfaznye Granitsy
https://journals.vsu.ru/kcmf/

Original articles

Research article
https://doi.org/10.17308/kcmf.2021.23/3438

Thermodynamic study of manganese tellurides by the electromotive force method

E. N. Orujlu[1]✉, Z. S. Aliev[2], Y. I. Jafarov[3], E. I. Ahmadov[3], M. B. Babanly[1,3]

[1]Institute of Catalysis and Inorganic Chemistry, Azerbaijan National Academy of Sciences, 113 H. Javid ave., Baku AZ-1143, Azerbaijan

[2]Azerbaijan State Oil and Industry University, 6/21 Azadləq ave., Baku AZ-1010, Azerbaijan

[3]Baku State University, 23 Z. Khalilov Street, Baku Az-1148 Azerbaijan

Abstract

The thermodynamic properties of manganese tellurides were determined using an electromotive force (EMF) method with a liquid electrolyte in a temperature range from 300 to 450 K. EMF measurements were performed using equilibrium samples taken from the two-phase regions, namely $MnTe_2$ + Te and MnTe + $MnTe_2$, of the Mn–Te system. The phase compositions of all samples were controlled with the X-ray diffraction (XRD) method. The partial molar functions of manganese in alloys, as well as the standard thermodynamic functions of the formation and standard entropies of MnTe and $MnTe_2$, were calculated. A comparative analysis of obtained results with literature data is performed.

Keywords: Electromotive force method, Thermodynamic properties, Manganese tellurides, MnTe, $MnTe_2$, Partial molar functions

Acknowledgements: the work has been carried out within the framework of the international joint research laboratory "Advanced Materials for Spintronics and Quantum Computing" (AMSQC) established between the Institute of Catalysis and Inorganic Chemistry of ANAS (Azerbaijan) and Donostia International Physics Center (Basque Country, Spain) and partially supported by the Science Development Foundation under the President of the Republic of Azerbaijan – Grant № EIF-GAT-5-2020-3(37)-12/02/4-M-02.

For citation: Orujlu E. N., Aliev Z. S., Jafarov Y. I., Ahmadov E. I., Babanly M. B. Thermodynamic study of manganese tellurides by the electromotive force method. *Kondensirovannye sredy i mezhfaznye granitsy = Condensed Matter and Interphases*. 2021;23(2): 273–281. https://doi.org/10.17308/kcmf.2021.23/3438

Для цитирования: Оруджлу Э. Н., Алиев З. С., Джафаров Я. И., Ахмедов Э. И., Бабанлы М. Б. Термодинамическое исследование теллуридов марганца методом электродвижущих сил. *Конденсированные среды и межфазные границы*. 2021;23(2): 273–281. https://doi.org/10.17308/kcmf.2021.23/3438

✉ Elnur N. Orujlu, e-mail: elnur.oruclu@yahoo.com

1. Introduction

Transition metal chalcogenides are considered promising candidates for spintronics, optoelectronics, and energy storage applications due to their unusual physical and chemical properties [1–4]. Among them, manganese tellurides are particularly interesting materials that provide a unique connection between semiconductivity and magnetism [5–7]. Recent studies show that ternary layered phases based on manganese telluride have the potential to combine two seemingly incompatible properties, topological insulation and magnetism, at the same time [8–12]. The first antiferromagnetic topological insulator [14] – $MnBi_2Te_4$ consists of a repetition of septuple blocks where magnetic MnTe bilayers are inserted into the quintuple Bi_2Te_3 layers periodically [15].

The knowledge of phase equilibria and reliable thermodynamic data of corresponding systems are crucially important for synthesizing novel complex phases and the development of modern sample-preparation techniques [16, 17].

Phase equilibria of the Mn-Te binary system have been investigated several times [18–20]. There exist two binary compounds of this type, namely MnTe and $MnTe_2$. Both compounds are formed by a peritectic reaction at 1424 and 1008 K, respectively. MnTe is a p-type semiconductor and crystallizes the "NiAs" type crystal structure, while $MnTe_2$ has a pyrite cubic crystal structure at low temperatures. MnTe undergoes several phase transformations from the low-temperature hexagonal phase to the high-temperature cubic phase [20].

An analysis of the literature shows that the first studies on the thermodynamic properties of manganese tellurides began in the late 19th century, and data obtained from both experimentally determined (calorimetry, vapor measurements, EMF) and model-calculated values have been collected in modern handbooks and electronic databases [21–31]. It should be noted that all previous studies, including those conducted by EMF, were performed in high-temperature ranges. An analysis of these works shows that the values of standard integral thermodynamic functions calculated from high-temperature measurements are significantly different from each other. Therefore, in order to obtain a more reliable set of standard thermodynamic functions, it is advisable to use experimental data obtained under conditions as close as possible to the standard.

Considering the above, the purpose of this work is a thermodynamic study of the Mn-Te system by EMF method with a liquid electrolyte in the temperature range from 300 to 450 K.

2. Experimental

To study the thermodynamic properties of the manganese-tellurium system, several compositions having 52, 60, 70, and 80 at% Te were synthesized from high purity (99.9999 % pure, Alfa Aesar and Sigma-Aldrich) elemental components in evacuated (10^{-2} Pa residual pressure) quartz tubes at 1300 K for 5 h. Glassy carbon crucibles were used to synthesize all samples to prevent the manganese reacting with quartz. All samples were subjected to annealing at 600 K for 240 h to reach an equilibrium state. The phase composition of the alloys was identified by means of differential thermal analysis (DTA) and powder X-ray diffraction (PXRD). DTA of the annealed alloys was carried out using the LINSEIS HDSC PT1600 system with a heating rate of 10 K/min. The temperature accuracy was better than 2 K. PXRD data collection was performed at room temperature on a Bruker D2 PHASER diffractometer using CuK_α radiation within $2\theta = 5^o–75^o$.

The concentration cell of

$$(-)\ \text{Mn (s.)} \ \Big|\ \begin{matrix}\text{liquid}\\ \text{electrolyte,}\\ Mn^{2+}\end{matrix}\ \Big|\ \begin{matrix}\text{(Mn in alloy)}\\ \text{(s.) (+)}\end{matrix} \qquad (1)$$

type was assembled for EMF measurements in the 300–450 K temperature interval.

A glycerol solution of KCl with the addition of 0.1 % $MnCl_2$ was used as an electrolyte. Glycerol electrolytes are successfully used for the low-temperature thermodynamic analysis of chalcogenide systems [32, 33]. In order to avoid having moisture and oxygen in the electrolyte, the glycerol was thoroughly dried and degassed under vacuum at ~450 K and anhydrous chemically pure KCl and $MnCl_2$ salts were used.

In a cell of type (1), metal manganese was used as a negative electrode, while the positive electrode was an annealed alloy of the Mn-Te system. The phase compositions of all the

indicated alloys and correspondence to the phase diagram were confirmed by the PXRD method. As an example, Fig. 1 shows powder diffraction patterns of two selected alloys from these regions. Both electrodes were prepared by pressing the piece of manganese and powdered alloys of the Mn-Te system on a molybdenum wire in the form of pellets weighing 0.5 g.

The electrochemical cell was constructed similar to that in [32,33], which allows measuring the EMF values of several electrodes relative to a reference electrode.

EMF measurements were performed using a Keithley 2100 6 1/2 Digit Multimeter. The first EMF equilibrium values were recorded after keeping the cell at ~360 K for 20–40 h. Values were thereafter obtained every 3–4 h after establishing the desired temperature. The system was considered to achieve an equilibrium state when the EMF values varied by less than 0.5 mV.

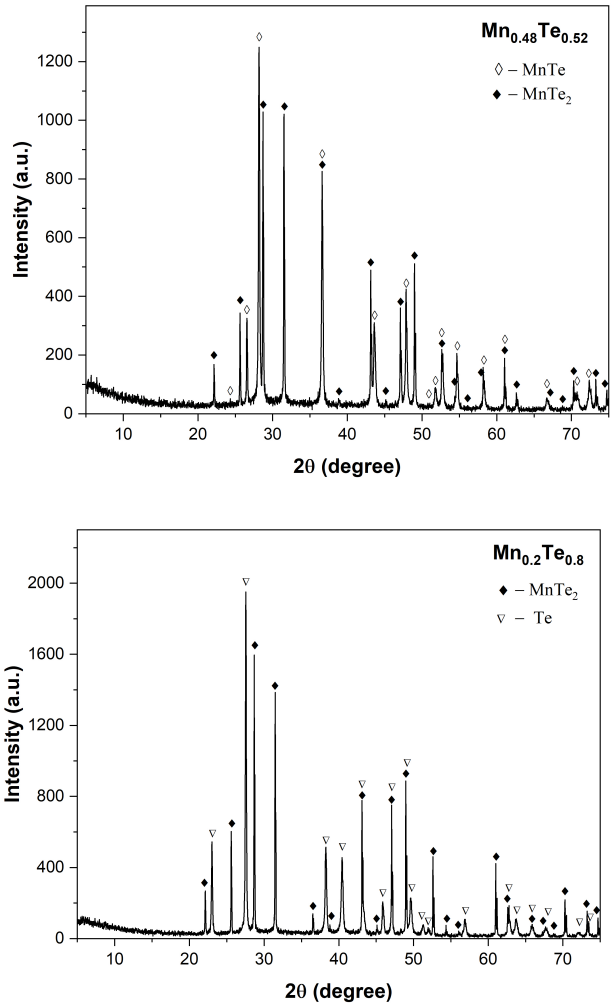

Fig. 1. PXRD patterns of the alloys from two-phase regions of the Mn-Te system

3. Results and discussion

The results of the EMF measurements of the concentration cell of type (1) confirms the existence of two-phase regions, namely MnTe+$MnTe_2$ and $MnTe_2$+Te in the Mn-Te system. The EMF isopleths at 400 K show that the EMF results in each two-phase region remain constant and change dramatically at the border (Fig. 2).

The temperature dependences of the EMF of type (1) cells for two-phase alloys are shown in Fig. 3. As can be seen, the EMF values increase linearly with increasing temperature. The linear relationship between EMF and temperature made it possible to consider the EMF measurement results using the least-squares method via computer software. Experimentally obtained data for temperature (T_i), EMF (E_i) and data associated with the calculation steps for both MnTe + $MnTe_2$ and $MnTe_2$ + Te phase regions of the Mn-Te system are listed in Tables 1 and 2.

We used the method of processing the results of the EMF measurements described in [34, 35]. The obtained linear equation of the type (2) are listed in Table 3 in the literature recommended form:

$$E = a + bT \pm t\left[\left(S_E^2 / n\right) + S_b^2 \cdot \left(T - \bar{T}\right)^2\right]^{1/2} \quad (2)$$

Here n is the number of pairs of E and T values; S_E and S_b – are dispersions of individual measurements of EMF and constant b; $\bar{T}$ – the average absolute temperature; t – the Student's t-test. At the confidence level of 95 %

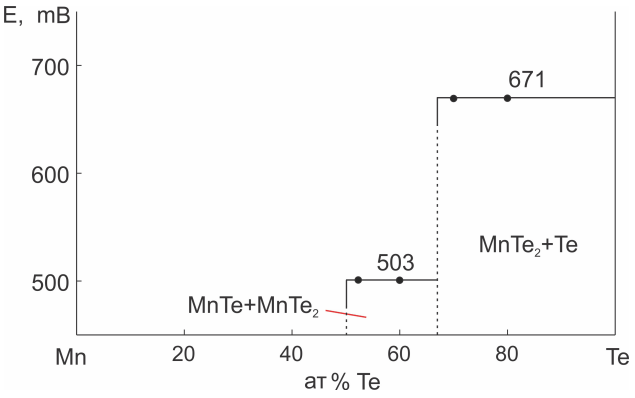

Fig. 2. The composition dependences of the EMF of type (1) cells at 400 K

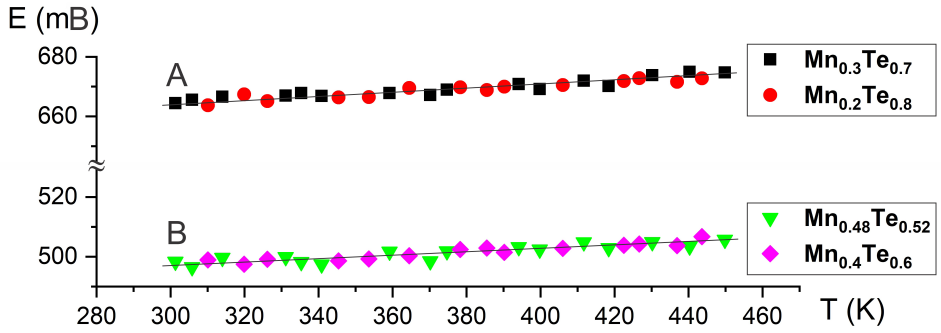

Fig. 3. The temperature dependences of EMF of the concentration cells type (1) for $MnTe_2$+Te (A) and MnTe+$MnTe_2$ (B) phase regions of the Mn-Te system

Table 1. Experimentally obtained data for the temperature (T_i), EMF (E_i) and data associated with the calculation steps for the $MnTe_2$+Te phase region of the Mn–Te system

T_i, K	E_i, mV	$T_i - \bar{T}$	$E_i(T_i - \bar{T})$	$(T_i - \bar{T})^2$	$\tilde{E}$	$E_i - \tilde{E}$	$(E_i - \tilde{E})^2$
301.3	664.41	−74.90	−49766.52	5610.51	664.53	−0.12	0.01
305.8	665.53	−70.40	−46855.53	4956.63	664.80	0.73	0.53
310.1	663.72	−66.10	−43874.10	4369.65	665.07	−1.35	1.82
314	666.54	−62.20	−41461.01	3869.25	665.31	1.23	1.52
319.9	667.36	−56.30	−37574.59	3170.07	665.67	1.69	2.86
326.2	665.13	−50.00	−33258.72	2500.33	666.06	−0.93	0.86
331.1	666.91	−45.10	−30079.86	2034.31	666.36	0.55	0.31
335.3	667.81	−40.90	−27315.66	1673.08	666.62	1.19	1.43
340.8	666.82	−35.40	−23607.65	1253.40	666.95	−0.13	0.02
345.4	666.35	−30.80	−20525.80	948.85	667.24	−0.89	0.79
353.6	666.46	−22.60	−15064.22	510.91	667.74	−1.28	1.64
359.2	667.82	−17.00	−11355.17	289.11	668.08	−0.26	0.07
364.5	669.54	−11.70	−7835.85	136.97	668.41	1.13	1.28
370.2	667.13	−6.00	−4005.00	36.04	668.76	−1.63	2.66
374.7	668.91	−1.50	−1005.59	2.26	669.04	−0.13	0.02
378.3	669.74	2.10	1404.22	4.40	669.26	0.48	0.23
385.5	668.82	9.30	6217.80	86.43	669.70	−0.88	0.77
390.2	669.92	14.00	9376.65	195.91	669.99	−0.07	0.00
394.1	670.82	17.90	12005.44	320.29	670.23	0.59	0.35
399.8	669.16	23.60	15789.95	556.80	670.58	−1.42	2.01
406	670.51	29.80	19978.96	887.84	670.96	−0.45	0.20
411.7	671.92	35.50	23850.92	1260.01	671.31	0.61	0.37
418.4	670.14	42.20	28277.67	1780.56	671.72	−1.58	2.50
422.5	671.81	46.30	31102.56	2143.38	671.97	−0.16	0.03
426.7	672.82	50.50	33975.17	2549.91	672.23	0.59	0.35
430.2	673.83	54.00	36384.57	2915.64	672.45	1.38	1.91
436.9	671.54	60.70	40760.24	3684.09	672.86	−1.32	1.74
440.3	674.92	64.10	43260.12	4108.38	673.07	1.85	3.43
443.6	672.73	67.40	45339.76	4542.31	673.27	−0.54	0.29
449.8	674.75	73.60	49659.35	5416.47	673.65	1.10	1.21
$\bar{T} = 376.2$	$\bar{E} = 669.129$		$\sum = 3798.11$	$\sum = 61813.79$			$\sum = 31.2$

Table 2. Experimentally obtained data for the temperature (T_i), EMF (E_i) and data associated with the calculation steps for the MnTe+$MnTe_2$ phase region of the Mn–Te system

T_i, K	E_i, mV	$T_i - \bar{T}$	$E_i(T_i - \bar{T})$	$(T_i - \bar{T})^2$	$\tilde{E}$	$E_i - \tilde{E}$	$(E_i - \tilde{E})^2$
301.3	498.36	−74.90	−37328.83	5610.51	497.29	1.07	1.14
305.8	496.52	−70.40	−34956.66	4956.63	497.54	−1.02	1.04
310.1	498.91	−66.10	−32979.61	4369.65	497.77	1.14	1.29
314	499.62	−62.20	−31078.03	3869.25	497.99	1.63	2.67
319.9	497.45	−56.30	−28008.09	3170.07	498.31	−0.86	0.74
326.2	499.16	−50.00	−24959.66	2500.33	498.65	0.51	0.26
331.1	499.91	−45.10	−22547.61	2034.31	498.92	0.99	0.98
335.3	498.23	−40.90	−20379.27	1673.08	499.15	−0.92	0.84
340.8	497.42	−35.40	−17610.33	1253.40	499.45	−2.03	4.11
345.4	498.61	−30.80	−15358.85	948.85	499.70	−1.09	1.19
353.6	499.24	−22.60	−11284.49	510.91	500.15	−0.91	0.82
359.2	501.72	−17.00	−8530.91	289.11	500.45	1.27	1.61
364.5	500.33	−11.70	−5855.53	136.97	500.74	−0.41	0.17
370.2	498.52	−6.00	−2992.78	36.04	501.05	−2.53	6.41
374.7	501.81	−1.50	−754.39	2.26	501.30	0.51	0.26
378.3	502.44	2.10	1053.45	4.40	501.49	0.95	0.90
385.5	502.91	9.30	4675.39	86.43	501.89	1.02	1.05
390.2	501.43	14.00	7018.35	195.91	502.14	−0.71	0.51
394.1	503.22	17.90	9005.96	320.29	502.35	0.87	0.75
399.8	502.43	23.60	11855.67	556.80	502.67	−0.24	0.06
406	502.81	29.80	14982.06	887.84	503.00	−0.19	0.04
411.7	504.82	35.50	17919.43	1260.01	503.31	1.51	2.27
418.4	502.91	42.20	21221.13	1780.56	503.68	−0.77	0.59
422.5	503.83	46.30	23325.65	2143.38	503.90	−0.07	0.01
426.7	504.24	50.50	25462.44	2549.91	504.13	0.11	0.01
430.2	504.91	54.00	27263.46	2915.64	504.32	0.59	0.34
436.9	503.73	60.70	30574.73	3684.09	504.69	−0.96	0.92
440.3	503.44	64.10	32268.83	4108.38	504.87	−1.43	2.06
443.6	506.72	67.40	34151.24	4542.31	505.05	1.67	2.77
449.8	505.71	73.60	37218.57	5416.47	505.39	0.32	0.10
$\bar{T}$ = 376.2	$\bar{E}$ = 501.38		$\sum$ = 3371.31	$\sum$ = 61813.79			$\sum$ = 35.89

Table 3. Temperature dependences of the EMF for the cell of type (1) for alloys of the Mn–Te in the temperature range of 300–450 K

Phase area	E, mV$= a + bT + t \cdot \tilde{S}_E(T)$
$MnTe_2$+Te	$646.03 + 0.0614T \pm 2\left[\frac{1.04}{30} + 1.7 \cdot 10^{-5}\left(T - 376.2\right)^2\right]^{1/2}$
MnTe+$MnTe_2$	$480.86 + 0.0546T \pm 2\left[\frac{1.2}{30} + 1.9 \cdot 10^{-5}\left(T - 376.2\right)^2\right]^{1/2}$

and n = 30, the Student's t-test ⩽ 2. Using the obtained equations of type (2) and the following thermodynamic expressions:

$$\Delta\bar{G}_{\mathrm{Mn}} = -zFE \quad (3)$$

$$\Delta\bar{H}_{\mathrm{Mn}} = -z\left[E - T\left(\frac{\partial E}{\partial T}\right)_P\right] = -zFa \quad (4)$$

$$\Delta\bar{S}_{\mathrm{Mn}} = -zF\left(\frac{\partial E}{\partial T}\right)_P = zFb \quad (5)$$

the partial molar functions of manganese in the alloys at 298 K were calculated. The results are given in Table 4.

According to the phase diagram of the Mn-Te system, the values of the partial molar functions can be considered thermodynamic functions of the following virtual cell reactions (all substances are solid) [34, 35]:

$$\mathrm{Mn} + 2\,\mathrm{Te} = \mathrm{MnTe_2} \quad (6)$$

$$\mathrm{Mn} + \mathrm{MnTe_2} = 2\,\mathrm{MnTe} \quad (7)$$

According to the (6) and (7) reaction equations, the standard thermodynamic functions of formation for both MnTe and $MnTe_2$ compounds are calculated using the following expressions:

$$\Delta_f Z^\circ_{\mathrm{MnTe_2}} = \Delta\bar{Z}_{\mathrm{Mn}} \quad (8)$$

$$\Delta_f Z^\circ_{\mathrm{MnTe}} = 0.5\Delta\bar{Z}_{\mathrm{Mn}} + 0.5\Delta_f Z^\circ_{\mathrm{MnTe_2}} \quad (9)$$

where $\Delta Z = \Delta G$ or ΔH. The standard entropy was calculated as:

$$S^\circ_{\mathrm{MnTe_2}} = \Delta\bar{S}_{\mathrm{Mn}} + S^\circ_{\mathrm{Mn}} + 2S^\circ_{\mathrm{Te}} \quad (10)$$

$$S^\circ_{\mathrm{MnTe}} = 0.5\Delta\bar{S}_{\mathrm{Mn}} + 0.5S^\circ_{\mathrm{Mn}} + 0.5S^\circ_{\mathrm{MnTe_2}} \quad (11)$$

In the calculations, the values of standard entropies of manganese (32.01±0.13 J/(mol·K)) and tellurium (49.50±0.21 J/(mol·K)) were taken from [25]. The errors were calculated by the error accumulation method. Available literature data and calculated values of the present work are summarized in Tables 5 and 6.

As can be seen from Tables 4 and 5, the values of standard Gibbs free energies of the formation of both MnTe and $MnTe_2$ compounds obtained by EMF measurements under standard conditions was determined with high accuracy. Our results show a good agreement with the results of high-temperature EMF (580–823 K) [21,22] studies and the combination of EMF with the DSC method [21]. These data are also well matched with the values of $\Delta_f G°$ of both compounds given in the databases [23–26].

A comparison of our results for $\Delta_f H°$ with all available literature data shows that the results calculated for the MnTe compound are in good agreement, except the old calorimetric data of Fabre [29]. For the $MnTe_2$ compound, our results are very close to the data obtained by a combination of EMF with DSC methods [21] and values recommended in databases [23–26]. At the same time, the values of the enthalpy of formation calculated by high-temperature EMF

Table 4. Relative partial thermodynamic functions of manganese in the alloys of the Mn–Te system (298 K)

Phase area	$-\Delta\bar{G}_{\mathrm{Mn}}$	$-\Delta\bar{H}_{\mathrm{Mn}}$	$-\Delta\bar{S}_{\mathrm{Mn}}$, J/(mol·K)
	kJ/mol		
$MnTe_2$+Te	128.20±0.07	124.67±0.30	11.86±0.79
MnTe+$MnTe_2$	95.95±0.08	92.79±0.32	10.54±0.85

Table 5. Standard thermodynamic functions of $MnTe_2$

$-\Delta_f G°$	$-\Delta_f H°$	$\Delta_f S°$	$S°$	Ref., Methods
kJ/mol		J/(mol·K)		
128.2±0.1	124.7±0.3	11.9±0.8	142.9±1.4	This work, EMF, 300-450 K
127.6±0.6	131.2±1.2	–12.1±4.2		[21], EMF, 594-723 K
127.5±0.6	125.4±1.8	7.8±5.1		[21], EMF with DSC, 298-723 K
124.3±1.0	119.4±1.8	16.5±3.3		[22], EMF, 723-823 K
129.7	125.5±4.2		145	[23,24], recommend.
127.6	123.4±3.5		145.0±0.4	[25,26], recommend.
	120.5	10.7		[27], modeling
			145.0	[28], DSC

Table 6. Standard thermodynamic functions of MnTe

$-\Delta_f G°$	$-\Delta_f H°$	$\Delta_f S°$	$S°$	Ref., Methods
kJ/mol		J/(mol·K)		
112.1±0.1	108.7±0.3	11.3±0.8	92.8±1.2	This work, EMF, 300-450 K
112.3±0.2	107.9±1.2	14.7±3.2		[21], EMF, 583–750 K
111.2±0.4	106.6±1.4	16.0±3.4		[21], EMF with DSC, 298–750 K
112.5±0.8	107.1±1.4	18.2±3.6		[22], EMF, 723–823 K
	94.2			[29], Calorimetry
	111.3±5.4			[30], Calorimetry
	109.6±8.0			[31], Vapor measurem.
112.1	108.4±2.9		94.0±1.7	[25], recommend.
112.0	108.4		93.7	[23, 24], recommend.
	109.2±3.8		93.7±1.7	[26], recommend.
	107.0	15.1		[27], modeling

measurements are significantly different from each other and our results. These discrepancies are especially clearly reflected in the values of $\Delta_f S°$ obtained in [21, 22, 27].

In summary, we note that our results on the standard entropies of both compounds are in good agreement with the literature data.

4. Conclusions

In the present paper, we report the results of a thermodynamic study of the Mn-Te system using the EMF method with a glycerol electrolyte in a temperature range from 300 to 450 K. According to the EMF measurements, the partial molar functions of manganese in two-phase regions, MnTe+$MnTe_2$ and $MnTe_2$+Te at 298 K, as well as the standard thermodynamic functions of the formation and standard entropies of MnTe and $MnTe_2$, were calculated. The new mutually consistent values of thermodynamic functions presented by us are the first experimental data obtained from EMF measurements under standard conditions. They supplement and clarify the previously obtained thermodynamic data for manganese tellurides.

Authors' Contributions

Orujlu E. N. – conducting experiments, processing data, writing text, final conclusions. Aliev Z. S. – X-ray diffraction analysis, discussion of results. Jafarov Y. I. – interpretation of the results. Ahmadov E. I. – review writing and text editing. Babanly M. B. – scientific supervision of research, concept of research, development of methodology.

Conflict of interests

The authors declare that they have no known competing financial interests or personal relationships that could have influenced the work reported in this paper.

References

1. Kau A. B., Two-dimensional layered materials: structure, properties, and prospects for device applications. *Journal of Materials Research*. 2014;29(3): 348–361. https://doi.org/10.1557/jmr.2014.6

2. Tedstone A. A., Lewis D. J., O'Brien P., Synthesis, properties, and applications of transition metal-doped layered transition metal dichalcogenides. *Chemistry of Materials*. 2016;28: 1965–1974. https://doi.org/10.1021/acs.chemmater.6b00430

3. Ali Z., Zhang T., Asif M., Zhao L., Hou Y., Transition metal chalcogenide anodes for sodium storage. *Materials Today*. 2020;35: 131–167. https://doi.org/10.1016/j.mattod.2019.11.008

4. Shang C., Fu L., Zhou S., Zhao J. Atomic Wires of transition metal chalcogenides: A family of 1D materials for flexible electronics and spintronics. *Journal of the American Chemical Society AU*. 2021:1(2); 147–155. https://doi.org/10.1021/jacsau.0c00049

5. Xu Y., Li W., Wang C., Chen Z., Wu Y., Zhang X., Li J., Lin S., Chen Y., Pei Y. $MnTe_2$ as a novel promissing thermoelectric material, *Journal of Materiomics*. 2018;4(3): 215–220. https://doi.org/10.1016/j.jmat.2018.04.001

6. Sreeram P. R., Ganesan V., Thomas S., Anantharaman M. R. Enhanced thermoelectric performance of nanostructured manganese telluride via antimony doping. *Journal of Alloys and Compounds*. 2020;836: 155374. https://doi.org/10.1016/j.jallcom.2020.155374

7. Basit A., Yang J., Jiang Q., Zhou Z., Xin J., Li X., Li S. Effect of Sn doping on thermoelectric properties

of p-type manganese telluride. *Journal of Alloys and Compounds*. 2019;777: 968–973. https://doi.org/10.1016/j.jallcom.2018.11.066

8. Mong R. S. K., Moore J. E., Magnetic and topological order united in a crystal. *Nature*. 2019;576: 390–392. https://doi.org/10.1038/d41586-019-03831-7

9. Tokura Y., Yasuda K., Tsukazaki A. Magnetic topological insulators. *Nature Reviews Physics*. 2019;1: 126–143. https://doi.org/10.1038/s42254-018-0011-5

10. Wu J., Liu F., Sasase M., Ienaga K., Obata Y., Yukawa R., Horiba K. Natural van der Waals heterostructural single crystals with both magnetic and topological properties. *Science Advances*. 2019;5(11): eaax9989. https://doi.org/10.1126/sciadv.aax9989

11. Estyunin D. A., Klimovskikh I.I., Shikin A.M., Schwier E.F., Otrokov M.M., Kimura A., Kumar S., Filnov S. O., Aliev Z. S., Babanly M. B., Chulkov E. V. Signatures of temperature driven antiferromagnetic transition in the electronic structure of topological insulator $MnBi_2Te_4$. *APL Materials*. 2020;8: 021105(1-7). https://doi.org/10.1063/1.5142846

12. Klimovskikh I. I., Otrokov M. M., Estyunin D., Eremeev S. V., Filnov S. O., Koroleva A., Shevchenko E., Voroshnin V., Rybkin A. G., Rusinov I. P., Blanco-Rey M., Hoffmann M., Aliev Z. S., Babanly M. B., Amiraslanov I. R., Abdullayev N. A., Zverev V. N., Kimura A., Tereshchenko O. E., Kokh K. A., Petaccia L., Santo G. D., Ernst A.,. Echenique P. M, Mamedov N. T., Shikin A. M., Chulkov E. V. Tunable 3D/2D magnetism in the $(MnBi_2Te_4)(Bi_2Te_3)_m$ topological insulators family. *npj Quantum Materials*. 2020;5(1): 1–9. https://doi.org/10.1038/s41535-020-00255-9

13. Shikin A. M., Estyunin D. A., Klimovskikh I. I., Filnov S. O., Schwier E. F., Kumar S., Miyamoto K., Okuda T., Kimura A., Kuroda K., Yaji K., Shin S., Takeda Y., Saitoh Y., Aliev Z. S., Mamedov N. T., Amiraslanov I. R., Babanly M. B., Otrokov M. M., Eremeev S. V., Chulkov E. V. Dirac gap modulation and surface magnetic interaction in axion antiferromagnetic topological insulator $MnBi_2Te_4$. *Scientific Reports*. 2020;10: 13226. https://doi.org/10.1038/s41598-020-70089-9

14. Otrokov M. M., Klimovskikh I. I., Bentmann H., Estyunin D., Zeugner A., Aliev Z. S., Gaß S., Wolter A. U. B, Koroleva A. V., Shikin A. M., Blanco-Rey M., Hoffmann M., Rusinov I. P., Vyazovskaya A. Y., Eremeev S. V., Koroteev Y. M., Kuznetsov V. M., Freyse F., Sбnchez-Barriga J., Amiraslanov I. R., Babanly M. B., Mamedov N. T., Abdullayev N. A., Zverev V. N., Alfonsov A., Kataev V., Büchner B., Schwier E. F., Kumar S., Kimura A., Petaccia L., Di Santo G., Vidal R. C., Schatz S., Kißner K., Ünzelmann M., Min C. H., Moser S., Peixoto T. R. F., Reinert F., Ernst A., Echenique P. M., Isaeva A., Chulkov E. V. Prediction and observation of an antiferromagnetic topological insulator. *Nature*. 2019;576: 416–422. https://doi.org/10.1038/s41586-019-1840-9

15. Aliev Z. S., Amiraslanov I. R., Nasonova D. I., Shevelkov A. V., Abdullayev N. A., Jahangirli Z. A., Orujlu E. N., Otrokov M. M., Mamedov N. T.,. Babanly M. B,. Chulkov E. V. Novel ternary layered manganese bismuth tellurides of the $MnTe\text{-}Bi_2Te_3$ system: Synthesis and crystal structure. *Journal of Alloys and Compounds*. 2019;789: 443–450. https://doi.org/10.1016/j.jallcom.2019.03.030

16. Babanly M. B., Chulkov E. V., Aliev Z. S.,. Shevelkov A. V., Amiraslanov I. R. Phase diagrams in materials science of topological insulators based on metal chalcogenides. *Russian Journal of Inorganic Chemistry*. 2017;62: 1703–1729. https://doi.org/10.1134/S0036023617130034

17. Babanly M. B., Mashadiyeva L. F., Babanly D. M., Imamaliyeva S. Z., Tagiev D. B., Yusibov Y. A. Some issues of complex studies of phase equilibria and thermodynamic properties in ternary chalcogenide systems involving Emf measurements (Review). *Russian Journal of Inorganic Chemistry*. 2019;64: 1649–1671. https://doi.org/10.1134/S0036023619130035

18. Abrikosov N. Kh., Dyul'dina K. A., Zhdanova V. V. Study of the Mn-Te System. *Izvestiya Akademii nauk SSSR, seriya Neorganicheskiye Materialy*. 1967;4: 1878–1884. (in Russ.)

19. Vanyarkho V. G., Zlomanov V. P., Novoselova A. V. Physicochemical study of manganese telluride. *Izvestiya Akademii nauk SSSR*, *seriya Neorganicheskiye Materialy*. 1969;6: 1257–1259. (in Russ.)

20. Schlesinger M. E. The Mn-Te (manganese-tellurium) system. *Journal of Phase Equilibria*. 1998;19(6): 591–596. https://doi.org/10.1361/105497198770341806

21. Vassilie V., Bykov M., Gambino M., Bros J. P. Thermodynamic investigation of the manganese-tellurium system. *Journal de Chimie Physique et de Physico-Chimie Biologique*. 1993;90(2): 463–476. https://doi.org/10.1051/jcp/1993900463

22. Loukachenko G., Polotskaya R. I., Duldina K. A., Abrikosov N. Kh. Thermodynamic properties of manganese-tellurium compounds. *Izvestiya Akademii nauk SSSR, seriya Neorganicheskiye Materialy*. 1971;7(5): 860–861. (In Russ.)

23. Barin I. *Thermochemical Data of Pure Substances,* Third Edition, VCH, 2008. 1936 p.

24. Mills K. C. *Thermodynamic data for inorganic sulphides, selenides and tellurides*, London, Butterworths; 1974. 845 p.

25. Iorish V. S., Yungman V. S. *Database of thermal constants of substances*. 2006. Available at: http://www.chem.msu.ru/cgi-bin/tkv.pl

26. Kubaschewski O., Alcock C. B., Spencer P. J. *Materials Thermochemistry*, Oxford: Pergamon Press Ltd; 1993. 363 p.

27. Chevalier P. Y., Fischer E., Marbeuf A. A thermodynamic evaluation of the Mn-Te binary system. *Thermochimica Acta*. 1993;223: 51–63. https://doi.org/10.1016/0040-6031(93)80119-U

28. Westrum E. F., Gronvold F., Manganese disulfide (hauerite) and manganese ditelluride. Thermal properties from 5 to 350°K and antiferromagnetic transitions. *The Journal of Chemical Physics*. 1970;52: 3820–3826. https://doi.org/10.1063/1.1673563

29. Fabre C. Thermal studies on the selenides. *Annales de chimie et de physique*. 1887;10: 472–550. (in French)

30. Morozova M. P., Stolyarova T. A. Formation enthalpy of manganese selenides and tellurides. *Vestnik Leningradskogo Universiteta, Seriya Fiziki i Khimii*. 1964;19(16): 150–153. (in Russ.)

31. Wiedemeier H., Sadeek H. Knudsen measurements ofthe sublimation of manganese (II) telluride. *High Temperature Science*. 1970;2: 252–258.

32. Imamaliyeva S. Z., Musayeva S. S., Babanly D. M., Jafarov Y. I., Tagiyev D. B., Babanly, M. B. Determination of the thermodynamic functions of bismuth chalcoiodides by EMF method with morpholinium formate as electrolyte. *Thermochimica Acta*. 2019;679: 178319(1-7). https://doi.org/10.1016/j.tca.2019.178319

33. Mashadiyeva L. F., Mansimova S. G., Babanly K. N., Yusibov Y. A., Babanly M. B. Thermodynamic properties of solid solutions in the PbSe–$AgSbSe_2$ system. *Russian Chemical Bulletin*. 2020;69: 660–664. https://doi.org/10.1007/s11172-020-2814-7

34. Morachevsky A. G., Voronin G. F., Geyderich V. A., Kutsenok I. B. *Elektrokhimicheskie metody issledovaniya v termodinamike metallicheskikh system.* [Electrochemical methods of investigation in hermodynamics of metal systems]. Moscow: Akademkniga Publ.; 2003. 334 p. Available at: https://elibrary.ru/item.asp?id=19603291 (In Russ.)

35. Babanly M. B., Yusibov Y. A. *Elektrokhimicheskie metody v termodinamike neorganicheskikh sistem* [Electrochemical methods in thermodynamics of inorganic systems]. Baku: BSU Publ.; 2011. 306 p.

Information about the authors

Elnur N. Orujlu, PhD student, Junior Researcher at the Institute of Catalysis and Inorganic Chemistry, Azerbaijan National Academy of Sciences, Baku, Azerbaijan; e-mail: elnur.oruclu@yahoo.com. ORCID iD: https://orcid.org/0000-0001-8955-7910.

Ziya S. Aliev, PhD in Chemistry, Assistance Professor, Azerbaijan State Oil and Industry University, Baku, Azerbaijan; e-mail: ziyasaliev@gmail.com. ORCID iD: https://orcid.org/0000-0001-5724-4637.

Yasin I. Jafarov, DSc in Chemistry, Associate Professor, Baku State University, Baku, Azerbaijan; e-mail: yasin.cafarov@hotmail.com. ORCID iD: https://orcid.org/0000-0002-6597-2252

Eldar I. Ahmadov, DSc in Chemistry, Professor, Baku State University, Baku, Azerbaijan; e-mail: eldar_akhmedov@mail.ru.

Mahammad B. Babanly, Corresponding Member of the Azerbaijan National Academy of Sciences, Deputy-director of the Institute of Catalysis and Inorganic Chemistry, Azerbaijan National Academy of Sciences, Baku State University, Baku, Azerbaijan; e-mail: babanlymb@gmail.com. ORCID iD: https://orcid.org/0000-0001-5962-3710.

Received 17 February 2021; Approved after reviewing 12 March 2021; Accepted 15 May 2021; Published online 25 June 2021

Edited and proofread by Simon Cox